Khalife Rana (Orcid ID: 0000-0001-7956-9707)

Optimization of the Nutritional Environment for Differentiation of Human Induced Pluripotent Stem Cells using Design of Experiments – A Proof of Concept

Patricia P. Esteban[2†], Hamza Patel[1], Farlan Veraitch[1], Rana Khalife[1*†]

[1] Department of Biochemical Engineering, University College London, Torrington Place, London, WC1E 7JE, UK

[2] College of Health & Life Sciences, School of Biosciences, Aston University, Aston Triangle, Birmingham, B4 7ET, UK

* Author to whom correspondence should be addressed: rana.khalife.13@ucl.ac.uk

[†]Patricia P. Esteban and Rana Khalife are joint first authors.

Abstract

The utilization of human pluripotent stem cells (hiPSCs) in cell therapy has a tremendous potential but faces many practical challenges, including costs associated with cell culture media and growth factors. There is an immediate need to establish an optimized culture platform to direct the differentiation of hiPSCs into germ layers in a defined nutritional microenvironment to generate cost-effective and robust therapeutics. The aim of this study was to identify the optimal nutritional environment by mimicking the *in vivo* concentrations of three key factors (glucose, pyruvate and oxygen) during the spontaneous differentiation of hiPSCs derived from cord blood, which greatly differ from the *in vitro* expansion and differentiation scenarios. Moreover, we hypothesized that the high glucose, pyruvate and oxygen concentrations found in

This article has been accepted for publication and undergone full peer review but has not been through the copyediting, typesetting, pagination and proofreading process which may lead to differences between this version and the Version of Record. Please cite this article as doi: 10.1002/btpr.3143

typical growth media could inhibit the differentiation of certain lineages. A design of experiments (DoE) was used to investigate the interaction between these three variables during the spontaneous differentiation of hiPSCs. We found that lower oxygen and glucose concentrations enhance the expression of mesodermal (Brachyury, KIF1A) and ectodermal (Nestin, β-Tubulin) markers. Our findings present a novel approach for efficient directed differentiation of hiPSCs through the manipulation of media components whilst simultaneously avoiding the usage of growth factors thus reducing costs.

Keywords: Human Induced Pluripotent Stem Cells, Germ Layer Differentiation, Design of Experiments.

Introduction

The field of stem cell research has expanded greatly since the discovery of induced pluripotent stem cells (iPSCs). Reprograming adult somatic cells into iPSCs helped overcoming the ethical and immunological barriers associated with the use of embryonic stem cells (ESCs) (Takahashi & Yamanaka 2006; Robinton et al. 2012; Meyer, 2008).

Yamanaka and his colleagues first reprogrammed mouse induced pluripotent stem cells (miPSCs) from adult mouse fibroblasts via the introduction into the cell of 4 key transcription factors (Yamanaka's factors): octamer-binding transcription factor 4 (OCT-4), sex determining region Y box 2 (SOX2), myelocytomatosis viral oncogene homologue (c-MYC) and Kruppel-like factor 4 (KLF4) (Takahashi & Yamanaka, 2006). Following this, human induced pluripotent stem cell (hiPSCs) was also generated by the addition of integrating retroviral vectors expressing the same genes (Takahashi &

Yamanaka, 2007). The discovery of hiPSCs led to the mitigation of ethical concerns related to hESCs (Meyer, 2008) and the advancement of autologous cell therapy. The use of iPSCs in regenerative medicine is diverse and ranges from the treatment of Parkinson's disease (Wernig et al., 2008; Kriks et al., 2011), spinal cord injury (Tsuji et al., 2010; Nori et al., 2011), platelet deficiency (Takayama et al., 2010) to retinal and macular de-generation (Okamoto and Takahashi, 2011). Moreover, patient-specific iPSCs are used as a model to understand several diseases like amyotrophic lateral sclerosis (ALS) (Dimos et al., 2008), Parkinson's disease (Devine et al., 2011), Alzheimer's disease (Yagi et al., 2011; Yahata et al., 2011), and schizophrenia (Brennand et al., 2011). Other iPSCs models have been generated for the treatment of adenosine deaminase deficiency-related severe combined immunodeficiency, Shwachman-Bodian-Diamond syndrome, Gaucher disease type II, Duchenne and Becker muscular dystrophy, Parkinson disease, Huntington disease, juvenile-onset type 1 diabetes mellitus, Down syndrome, and Lesch-Nyhan syndrome (Park et al., 2008).

One of the main challenges in the implementation of hiPSCs in clinical trials and scale-up manufacturing is cost, due to the growth factor requirements, especially for large-scale production. Thus, there is an urgent need to establish optimal and economically viable growth conditions to direct the differentiation of pluripotent stem cells in a defined nutritional microenvironment.

In addition to the economic issues, nutritional microenvironments can have an impact on cell type authenticity. Any perturbation in the energy metabolism could affect self-renewal, differentiation and stem cell fate as the metabolism of pluripotent stem cells

is different from their differentiated counterparts (Kondoh et al., 2007; Varum et al., 2011; Sperber et al., 2015; Vernardis et al., 2017).

The analysis of the effects of the nutritional environment and energy metabolism on the differentiation of pluripotent stem cells (iPSCs and ESCs) *in vitro* is underpinned by the understanding of the embryo environment *in vivo*. During early development, the embryo is exposed to nutrients via vascular perfusion of the fallopian tube (Dickens et al., 1995; Gardner et al., 1996; Tay et al., 1997). The embryo resides in a low oxygen niche environment (Fischer and Bavister, 1993) and a switch from oxidative phosphorylation to glycolysis is sensed (Leese and Barton, 1984). The embryo is exposed to low glucose concentration during early development (Dickens *et al.*, 1995; Gardner *et al.*, 1996; Tay *et al.*, 1997), and it is known that the average oxygen levels in the human uterine surface change from 2.4% at week 7-10 up to 7-8 % after the maternal blood flows to the foetus in week 11 (Rodesch *et al.*, 1992). Thus, the *in vivo* concentrations of key nutrients that could have an effect on the metabolism such as oxygen, glucose and pyruvate, are much lower than the *in vitro* differentiation conditions (Fischer and Bavister, 1993; Dickens et al., 1995; Gardner et al., 1996; Tay et al., 1997; Y. Yang et al., 2016). In this study, the *in vivo* microenvironment was reproduced and compared to laboratory conditions and complete deprivation (0% oxygen, 0 mM glucose, 0 mM pyruvate).

To allow the investigation of three factors (oxygen, glucose and pyruvate concentrations) with multiple concentrations in parallel, a design of experiments (DoE) approach was chosen to provide insights on the experimental space and interactions within factors (Lundstedt *et al.*, 1998; Montgomery, 2012).

The ability of DoE to generate an algorithmic model aids in the optimization of experimental conditions by highlighting any interaction that might exist between the factors while reducing the number of experiments (Lundstedt *et al.*, 1998; Montgomery, 2012). DoE has been applied in fields such as engineering (Thielman and Ge, 2006; Ariffin *et al.*, 2009), drug optimization (Singh *et al.*, 2005; Martinello *et al.*, 2006), microbiology (Mannall, Titchener-Hooker and Dalby, 2007; Esteban *et al.*, 2014) and in the optimization of the pluripotent stem cell media (Marinho, Chailangkarn and Muotri, 2015). Nevertheless, to date, there are no studies that investigate the effect of nutritional microenvironment on germ layer formation using DoE. As a result, the aim of this study was to investigate whether mimicking the natural environment or depriving the oxygen, glucose and pyruvate could enhance or affect germ layer formation.

Material and Methods

Human Induced Pluripotent Stem Cell Expansion and Differentiation

Episomal hiPSC (Cord blood) line was purchased from Life Technologies (Lot number 1648638) and generated using cord blood-derived CD34+ progenitors with seven episomally expressed factors (OCT-4, SOX2, KLF4, c-MYC, NANOG, LIN28, and SV40 T). Mycoplasma testing was routinely performed and genetic instability of this cell line was assessed via karyotyping at passages 40 and 63. This line was first grown on mouse feeders and then adapted to a feeder-free system. These cell lines were cultured in Essential 8 medium (Thermo-Fisher Scientific) on vitronectin VTN-N (Thermo-Fisher Scientific) coated flasks. The differentiation of hiPSCs was performed through single cell suspension differentiation. hiPSCs were washed with PBS before adding TrypLE (Gibco) and incubating for 5 minutes at 37^{o}C, differentiation media was

added, and cells were passed through a 40 µm cell strainer (BD Bioscience), then centrifuged at 1,250 rpm for 5 minutes. After counting, cells were seeded as single cell in a 12-well plate pre-coated with reduced growth factor Matrigel (BD Bioscience) at a density of $0.8x10^5$ cells/mL. Differentiation was induced by treating hiPSCs with DMEM-F12 (Gibco, catalogue number 11320033) and customized DMEM-F12 for other conditions. Customized media was produced, which did not contain glucose, pyruvate and glutamine. The media was supplemented with 20% knockout serum replacement media (Gibco), 1% Glutamax (Gibco), 1% non-essential amino acids (Gibco) and 0.1 β-mercaptoethanol (Gibco) and 1 ng/mL of Rho Kinase Inhibitor (ROKi) (Millipore). In conditions were cells were cultured at low oxygen tension, nitrogen was introduced into the incubators and sensors were used to confirm the desired oxygen tension. Additionally, media was primed at low oxygen levels before adding it to the differentiated cells. Cells were differentiated for 4 days in the different environmental conditions.

Cell number quantification

Trypan blue exclusion method was used in order to assess cell numbers and viability. Cells were detached from the 12-well plate using TrypLE and run on a Vi-Cell counter (Beckman Coulter).

Phase contrast microscopy for cell morphology

Phase contrast microscopy pictures of differentiated iPSCs derived from single cells in different conditions were taken using Evos® XL (Thermo-Fisher Scientific) as an imaging system.

Gene expression by Real Time Polymerase Chain Reaction (RT-PCR)

Gene expression after differentiation of hiPSCs was studied for endodermal markers (Sox17, FOXA2 and CXCR4), mesodermal markers (Brachyury and KIF1A), and ectodermal markers (Nestin, β-Tubulin) via real time polymerase chain reaction (RT-PCR). Firstly, RNA was extracted using RNeasy Micro Kit (Qiagen) as per manufacturer's instructions. At the end of the manufacturer's protocol, 40 µl of RNA samples diluted in RNAse-free water were obtained, and quantification was performed on a spectrophotometer (NanoDrop ND-1000, Thermo-Fisher Scientific) by measuring the absorbance at 260/280 nm. The synthesis of complementary deoxyribonucleic acid (cDNA) was then performed using a QuantiTect Reverse Transcription Kit (Qiagen) as per manufacturer's instructions. cDNA was obtained by first eliminating any genomic DNA contaminant by the addition of gDNA Wipeout buffer (Qiagen), which was added to up to 1µg of mRNA, then topped up to a final volume of 14 µl with RNAse free water. The mixture was incubated at 42°C for 2 minutes in a thermocycler (Bio-Rad). Furthermore, a master mix of Primer Mix Quantiscript, RT buffer and Quantiscript Reverse Transcriptase were added to the template RNA (total volume of 20 µl). The samples were run at 42°C for 15 minutes then at 95°C for 3 minutes and stored at -20°C. The cDNA synthesised from the previous step was mixed with Quantitect SYBR Green PCR Kits (Qiagen), Quantitect pre-validated primer assay, as shown in Table 1, and RNAse-free water to a total volume of 25µl, and then loaded in triplicate in Hard-Shell Low Profile Thin-Wall 96 Well Skirted PCR plates (Bio-Rad) and run on a Bio-Rad CFX 96 Connect Real-Time PCR machine for 40 cycles.

The polymerase chain reaction was performed screening for differentiation and pluripotent genes along with a house-keeping gene (β-Actin). The C_t values were taken

from the Bio-Rad CFX Manager 3.0 and fold changes were calculated from the normalized relative expression ($\Delta\Delta C_t$) using the Equation 1 (K. Livak)

$$Fold\ Change = 2^{-\Delta\Delta C_t} \qquad Eq.1$$

Where:

$$2^{-\Delta\Delta C_t} = \left[(C_t\ gene\ of\ interest - C_t\ internal\ control)_{sample\ A} - (C_t\ gene\ of\ interest - C_t\ internal\ control)_{sample\ B}\right]$$

Design of Experiments

To determine to optimal nutritional environment for each of the germ layers, a combination of the relative concentrations of glucose, pyruvate and oxygen in laboratory, physiological and deprivation environments (as shown in Table 2) was studied. A full factorial design comprising a set of 27 different conditions was generated in Design-Expert® v10 DoE software (Stat-Ease, Inc., Minnesota, USA) to allow the estimation of all possible interactions. The initial differentiation protocol was set for 7 days since the formation of *in vivo* germ layers occurs one week after gestation. As preliminary data (not shown) showed low viability in some conditions while expressing high gene expression, the differentiation time was shortened to 4 days. Glutamine levels were not measured as Glutamax was supplemented in the media because it is more stable than Glutamine.

The 27 different combinations of the three factors (oxygen, pyruvate and glucose concentrations) were tested for germ layer gene expression along with the cell counts. Differentiation of hiPSCs in each condition was performed in triplicate and the data generated from the RT-PCR during the 4 days of the differentiation process was fed back into the design software. Data for each response factor was transformed as appropriate in order to approximate a normal distribution, log fold gene expression was calculated to reduce the difference in the orders of magnitude between the expression of different gene markers (Guy et al, 2013). An automatic model selection tool was used to keep only significant terms in the model, as well as maximizing the resulting regression function of the model. The criterion used was backward p-value selection, set at a cut-off value of 0.1. ANOVA was used to analyze the reduced model to ensure statistical parameters were within the appropriate statistically significant limits. From the ANOVA analysis, F-values for all models were large enough to indicate adequate signal and reject the effect of noise. Overall, outputs from the ANOVA analysis suggested the models for all responses were significant. Using the gene expression for each of the germ layers and viable cell counts, a predictive mathematical model was generated to determine the best condition for the enhancement of each germ layer.

Statistical Analysis

The significance of the differences in the expression markers was tested using one-way ANOVA with Dunnett test and multiple comparisons for all conditions compared to the laboratory levels as control. The significance of differences in the expression of genes over time at complete deprivation, physiological levels and laboratory conditions was assessed using two-way ANOVA with multiple comparisons. Differences with p-

values < 0.05 are labeled with an asterisk (*); differences with p-values < 0.001 are labeled with four asterisks (****).

Results and Discussion

Glucose deprivation enhanced endodermal lineage formation

Monolayer single cell differentiated hiPSCs (cord blood) were cultured in 27 different conditions with varying levels of oxygen, glucose and pyruvate concentrations as shown in Table 2. Design Expert v10 DoE software (Stat-Ease, Inc., Minnesota, USA) was used to analyse the response factors from this study. The software yielded significant models for SOX17 and CXCR4 at days 3 and 4, thus FOXA2 was not presented in the contour maps shown in Figure 1. Oxygen was found to have no significant effect and was thus removed from the model by backward p-value elimination. The individual gene expression for all conditions was analysed and compared to the laboratory levels as control using one-way ANOVA with Dunnett test and multiple comparisons for quantification (data not shown). Additionally, a detailed analysis using two-way ANOVA with multiple comparisons of the expression of endodermal genes over time at complete deprivation, physiological levels and laboratory conditions can be seen in Figure 2 to account for time and concentration effects.

No significant differences were found in the expression of the early differentiation marker SOX17 or the late differentiation marker FOXA2 when compared to the control for any of the 27 conditions during the first day; however, the expression of CXCR4 was slightly higher at 0% oxygen tensions (data not shown). These findings are corroborated by the literature, and CXCR4 increased expression by hypoxia has

previously been shown to be driven by Hypoxia-Inducible Factor 1 (HIF-1α) (Staller et al., 2003).

On day 2, marginally higher SOX17 expression was seen when cells were exposed to deprived glucose media while maintaining the laboratory oxygen (20%) and pyruvate levels (0.14 mM) (Figure 2). This effect of glucose removal on SOX17 expression was seen clearly at days 3 and 4 (Figures 2C and 2D), being significantly higher at complete depletion of glucose than both at physiological and laboratory levels at day 3 (p-value = 0.0021 and 0.0041 respectively) and day 4 (p-value < 0.0001) as can be observed in Figure 2A. The depletion of glucose induces downregulation of the pluripotency marker OCT4 via oxidation without causing apoptosis (Marsboom et al., 2016), which is supported by our findings on cell viability (Figure 8). As a result of this reduction in OCT4 activity, endoderm-associated genes such as SOX17 are increasingly expressed (Hay et al., 2004).

The impact of complete deprivation on the expression of the late endodermal marker FOXA2 was seen on day 3 and to a larger extent on day 4, as shown in Figure 2B. It is reasonable to assume that, indeed, FOXA2 would be overexpressed in the absence of glucose, since this transcription factor is responsible for activating lipid metabolism and ketogenesis (von Meyenn et al., 2013).

Expression of CXCR4 was enhanced only at 20% O_2, 0 mM glucose; 0% O_2, 0 mM glucose, and 0% O_2, 17.50 mM glucose in the 4 days of differentiation (Figure 1C, D). Interestingly, the levels of CXCR4 in hiPSCs grown in physiological and deprivation conditions compared to their counterparts in the laboratory environment are consistently higher for all time points, yielding significant differences (p-value < 0.0001) both at day 3 and day 4 (Figure 2C) due to the overexpression of HIF-1α,

which in turn stabilises CXCR4 mRNA. This has been reported in various types of cancer niches (Guo et al., 2014).

Increasing the oxygen tension to 20% while keeping iPSCs deprived of glucose and under 0.14 mM pyruvate seems to increase the expression of endodermal markers even at day 4 as seen in Figure 1 (B, D) (1,700-fold increase of Sox17, and 80-fold increase of CXCR4). This effect is more pronounced than when hiPSCs are exposed to the same conditions with higher pyruvate concentration (0.50 mM), since the presence of exogenous pyruvate potentiates the differentiation of stem cells towards mesodermal lineages (Song et al., 2019).

Depleting glucose from media whilst keeping the physiological environmental levels of oxygen and pyruvate (2%, 0.14 mM respectively) enhances all endodermal markers from day 2 onwards (Figures 1,2). The deprivation of all three factors induced endodermal expression with a maximum of ~500-fold increase of SOX17 and ~40-fold increase of CXCR4 at day 3 without inducing the definitive endodermal marker (FOXA2) (Figure 2). We found that culturing hiPSCs in glucose-deprived media enhanced the endodermal gene expression while maintaining normal oxygen and pyruvate levels. Previous studies reported that low glucose has been shown to stimulate the commitment of human hematopoietic stem cells to the erythroid lineage (Oburoglu et al., 2014) and maturation of MSCs (Farrell et al., 2015).

There are several studies that focus on the effect of glucose concentration on the proliferation of mouse embryonic stem cells (mESCs) (Kim, Heo and Han, 2006), human bone marrow-derived MSC (Li et al., 2007), human hematopoietic stem cell differentiation (Oburoglu et al., 2014) and mesenchymal stem cells (MSC) (Stolzing, Coleman and Scutt, 2006; Dhanasekaran et al., 2013), yet, to date, there is no

evidence of the combined effect of oxygen, glucose and pyruvate and their interaction on germ layer formation without the addition of growth factors in the differentiation media.

Mesodermal differentiation was enhanced at low oxygen and glucose levels

Deprivation or exposing the cells to pyruvate did not have a significant effect on the mesodermal gene expression (Brachyury and KIFl1A) during the 4 days of differentiation thus pyruvate was removed from the model by backward p-value elimination. Expression of Brachyury was increased only on the edges of the contouring area (Montgomery, 2012) as seen in Figures 3D, when the oxygen was the lowest or the highest. Further quantification in Figure 4A shows that Brachyury was overexpressed both in deprivation and physiological conditions as opposed to laboratory conditions. The expression of KIFl1A was increased with lower oxygen tensions at all time points (Figure 4B). Moreover, glucose depleted media had an effect on the expression of KIFl1A compared to laboratory and physiological conditions, particularly on day 4 as demonstrated on Figure 4B (p-value < 0.0001). Lower oxygen tension (0-2%) somehow enhanced the expression of Brachyury and KIF1A in the 4 days of differentiation (Figure 3D). The contour area for mesodermal expression generally did not show noticeable differences in the gene expression for the 27 condition at day 1 and day 2 (data not shown), but clearly defined optimal conditions were observed at days 3 and 4 (Figure 3), with high expression of both markers at low oxygen tension. The combined effect of lower oxygen and glucose levels for the enhancement of mesodermal lineages is demonstrated in Figure 4. During differentiation, higher concentrations of pyruvate direct mesoderm and endoderm

lineage specification, mainly in oxygen and glucose-deprived environments as seen in Figures 1 and 3, which is supported by the literature (Song et al., 2019).

High oxygen levels decreased ectodermal gene expression

An analogous analysis was performed for ectodermal gene expression, and a quadratic model was fitted for ectodermal markers. The contour plots and analysis of gene expression over time at complete deprivation of glucose and pyruvate, physiological levels of these components and laboratory concentrations can be seen in Figures 5 and 6 respectively. As the pyruvate concentration was increased from 0 mM to 0.50 mM, the expression of ectodermal markers (Nestin and Tubulin 3) did not change when the cells were exposed to 0mM Glucose (Figure 5,6). Moreover, the expression of Tubulin 3 was higher when

hiPSCs were cultured at low oxygen tension (0%) during the 4 days. The general observed pattern in the ectodermal expression was that upon increasing the glucose and oxygen levels, the level of expression of Nestin and Tubulin 3 decreased – this can be observed in Figure 7, where for all time points the expression of both markers was significantly higher to various degrees at deprivation and physiological conditions, where the concentrations are lower than in the laboratory environment. Differentiating hiPSCs at 0% O_2 and 0 mM glucose also induced ectodermal markers with a maximum gene expression at day 3 (Figure 5-7).

We found that oxygen and glucose deprivation enhanced the ectodermal and mesodermal germ layer formation from the second day after the start of the differentiation process. The effect of oxygen deprivation alone has been shown in the literature for differentiated human ESCs or mESCs, where lower oxygen tension

stimulated the formation of mesoderm (Khan, Adesida and Hardingham, 2007; Koay and Athanasiou, 2008; Stacpoole et al., 2013) and ectodermal precursors (Mondragon-Teran, Lye and Veraitch, 2009; Mondragon-Teran et al., 2011).

The effect of glucose and oxygen levels on cell viability and cell morphology

Cell viability of hiPSCs was assessed via trypan blue exclusion method and is reported as a function of oxygen, glucose and pyruvate levels over time in Figure 8. Culturing hiPSCs in laboratory conditions led to the highest cell counts for all time points. As expected, stressing hiPSCs through exposure to deprived glucose and oxygen environments had an impact on cell viability (Park et al., 2019). Although higher gene expression was observed in some extreme conditions for each germ layer, lower viabilities were found. In general, low pyruvate concentrations (< 0.14 mM) promoted higher cell viability regardless of the concentration of glucose. For all levels of oxygen, reducing the concentration of glucose had a negative effect on viable cell counts. Despite subjecting hiPSCs to various conditions, including extreme deprivation of nutrients and oxygen, the morphology of the cells was found to be normal and healthy in appearance as shown in Figure 9.

Germ layer optimisation and model predictability

For each germ layer, the numerical optimisation tool in Design Expert was used to find the optimal set of conditions that maximised both gene expression and viable cell density. The numerical optimisation tool combines the desired goal of several response factors into an overall model desirability, which ranges from zero to one (with 1 having the highest desirability), thus the best condition retrieved from the model should have the highest model desirability.

The optimal set of conditions that achieved the highest desirability for each germ layer are summarised in Table 3. The output from the optimisation is also illustrated graphically in Figure 10. In summary, the enhancement of endodermal lineage gene expression occurred at low glucose levels, while low oxygen and glucose enhanced the mesodermal and ectodermal gene expression.

The effect of glucose addition on the predictive endoderm model

To test the optimised condition generated by the predictive model for endodermal linage (Table 3), cells were cultured in 0.10 mM glucose media while maintaining laboratory conditions for oxygen and pyruvate (20% and 0.5 mM respectively). Furthermore, to establish whether glucose deprived cells could proliferate and retain their high endodermal gene expression after the 3-day starvation period, media containing glucose was added to maintain the cells from day 4 onwards. The glucose deprived cells were able to proliferate and maintain high endodermal gene expression even 23 days post starvation (Figure 11, D). The endodermal gene expression of Sox 17 and CXCR4 decreased significantly after the glucose addition while the expression of FOXA2 remained unchanged (Figure 11, A). While there was no significant change in the ectodermal (Tubulin and Pax6) and mesodermal (Brachyury and KIFlA) expression as seen in Figure 11, B-C. The addition of glucose helped in the proliferation of the differentiated cells while maintaining its phenotype.

Conclusion

Despite technological advances, there are still numerous challenges in the production of large quantities of clinical grade iPSCs for cell therapies. The differentiation process

into any lineage is hindered by several bioprocess challenges, both upstream and downstream. If differentiation at scale is desired, high costs associated with the need for growth factors and other media components make manufacturing processes unaffordable. Optimizing differentiation is therefore a key step in scaling-up, and this can be achieved by applying the existing in-depth understanding of early differentiation of the embryo *in vivo*. During early embryo development, the levels of oxygen and metabolites are lower than in laboratory conditions; thus, the initial aim of this study was to investigate the impact of oxygen and nutrients on hiPSC proliferation and differentiation. We found that glucose deprivation enhanced endodermal lineage formation, particularly at physiological levels of oxygen and pyruvate. Mesodermal and ectodermal differentiation were enhanced in oxygen and glucose-deprived environments. These results informed our predictive model, which provides a novel approach for the efficient and cost-effective directed differentiation of iPSCs. Validation of the model and modification of simple growth parameters can allow the achievement of optimal differentiation pathways, providing the basis for a potential scale-up platform where differentiation is merely directed by varying concentrations of glucose, oxygen and pyruvate in the media.

Acknowledgments

The authors would like to acknowledge UCL's Department of Biochemical Engineering for funding this project.

Author Contributions

Patricia P. Esteban: writing-original draft; writing-review; formal analysis and editing. **Hamza Patel**: data acquisition. **Farlan Veraitch**: methodology; supervision.

Rana Khalife: Conceptualization; investigation; methodology; validation; writing-original draft; writing-review and editing; formal analysis.

Conflict of Interest

The authors declare no conflict of interest.

References

Ariffin, M. et al. (2009). An optimise drilling process for an aircraft composite structure using design of experiments. *Scientific Research and Essays*, 4(10), 1109–1116.

Brennand, K. J. et al. (2011). Modelling schizophrenia using human induced pluripotent stem cells. *Nature*, 473(7346), 221–225. *doi*: 10.1038/nature09915.

Devine, M. J. et al. (2011). Parkinson's disease induced pluripotent stem cells with triplication of the α-synuclein locus. *Nature Communications*, 2(1). *doi*: 10.1038/ncomms1453.

Dhanasekaran, M. et al. (2013). Effect of high glucose on extensive culturing of mesenchymal stem cells derived from subcutaneous fat, omentum fat and bone marrow. *Cell Biochemistry and Function*, 31(1), 20–29. *doi*: 10.1002/cbf.2851.

Dickens, C. J. et al. (1995). Physiology: Human tubal fluid: Formation and composition during vascular perfusion of the fallopian tube. *Human Reproduction*, 10(3), 505–508. *doi*: 10.1093/oxfordjournals.humrep.a135978.

Dimos, J. T. et al. (2008). Induced pluripotent stem cells generated from patients with ALS can be differentiated into motor neurons. *Science*, 321(5893), 1218–1221. doi: 10.1126/science.1158799.

Esteban, P. P. et al. (2014). Enhancement of the antimicrobial properties of bacteriophage-K via stabilization using oil-in-water nano-emulsions. *Biotechnology Progress*, 30(4), 932–944. *doi*: 10.1002/btpr.1898.

Farrell, M. J. et al. (2015). Functional consequences of glucose and oxygen deprivation on engineered mesenchymal stem cell-based cartilage constructs. *Osteoarthritis and Cartilage*, 23(1), 134–42. *doi*: 10.1016/j.joca.2014.09.012.FUNCTIONAL.

Fischer, B. and Bavister, B. D. (1993). Oxygen tension in the oviduct and uterus of rhesus monkeys, hamsters and rabbits. *Journal of reproduction and fertility*, 99, 673–679. *doi*: 10.1530/jrf.0.0990673.

Gardner, D. K. et al. (1996). Environment of the preimplantation human embryo in vivo: metabolite analysis of oviduct and uterine fluids and metabolism of cumulus cells. *Fertility and Sterility*, 65(2), 349–353. *doi:* 10.1016/S0015-0282(16)58097-2.

Guo, M. et al. (2014). Hypoxia Promotes Migration and Induces CXCR4 Expression via HIF-1α Activation in Human Osteosarcoma. *PLOS ONE*, 9(3): e90518.

Hay, D. C., Sutherland, L., Clark, John and Burton, T. (2004). Oct-4 Knockdown Induces Similar Patterns of Endoderm and Trophoblast Differentiation Markers in Human and Mouse Embryonic Stem Cells. *Stem Cells*, 22: 225-235.

Khan, W. S., Adesida, A. B. and Hardingham, T. E. (2007). Hypoxic conditions increase hypoxia-inducible transcription factor 2alpha and enhance chondrogenesis in stem cells from the infrapatellar fat pad of osteoarthritis patients. *Arthritis research & therapy*, 9(3), R55. *doi*: 10.1186/ar2211.

Kim, Y. H., Heo, J. S. and Han, H. J. (2006). High glucose increase cell cycle regulatory proteins level of mouse embryonic stem cells via PI3-K/Akt and MAPKs signal pathways. *Journal of Cellular Physiology*, 209(1), 94–102. *doi*: 10.1002/jcp.20706.

Koay, E. J. and Athanasiou, K. a (2008). Hypoxic chondrogenic differentiation of human embryonic stem cells enhances cartilage protein synthesis and biomechanical functionality. *Osteoarthritis and cartilage*, 16(12), 1450–1456. *doi*: 10.1016/j.joca.2008.04.007.

Kondoh, H. et al. (2007). A High Glycolytic Flux Supports the Proliferative Potential of Murine Embryonic Stem Cells. *Antioxidants & Redox Signaling*, 9(3). *doi*: 10.1089/ars.2006.1467.

Kriks, S. et al. (2011). Dopamine neurons derived from human ES cells efficiently engraft in animal models of Parkinson's disease. *Nature*, 480, 547-551. *doi*: 10.1038/nature10648.

Leese, H. J. and Barton, A. M. (1984). Pyruvate and glucose uptake preimplantation embryos. *Journal of Reproduction and Fertility*, 72, 9–13. *doi*: 10.1530/jrf.0.0720009.

Li, Y. M. et al. (2007). Effects of high glucose on mesenchymal stem cell proliferation and differentiation. *Biochemical and Biophysical Research Communications*, 363(1), 209–215. *doi*: 10.1016/j.bbrc.2007.08.161.

Lundstedt, T. et al. (1998). Experimental design and optimization. *Chemometrics and Intelligent Laboratory Systems*, 3–40. *doi:* 10.1016/S0169-7439(98)00065-3.

Mannall, G. J., Titchener-Hooker, N. J. and Dalby, P. A. (2007). Factors affecting protein refolding yields in a fed-batch and batch-refolding system. *Biotechnology and Bioengineering,* 97(6), 1523–1534. *doi*: 10.1002/bit.21377.

Marinho, P. A., Chailangkarn, T. and Muotri, A. R. (2015). Systematic optimization of human pluripotent stem cells media using Design of Experiments. *Scientific Reports*, 5. *doi*: 10.1038/srep09834.

Martinello, T. et al. (2006). Optimization of poorly compactable drug tablets manufactured by direct compression using the mixture experimental design. *International Journal of Pharmaceutics*, 322(1–2), 87–95. *doi*: 10.1016/j.ijpharm.2006.05.034.

Marsboom, G. et al. (2016). Glutamine Metabolism Regulates the Pluripotency Transcription Factor OCT4. *Cell Reports*, 16(2): 323-332.

Meyer, J. R. (2008). The significance of induced pluripotent stem cells for basic research and clinical therapy. *Journal of Medical Ethics*, 34(12), 849–851. *doi*: 10.1136/jme.2008.024786.

Mondragon-Teran, P. et al. (2011). The full spectrum of physiological oxygen tensions and step-changes in oxygen tension affects the neural differentiation of mouse embryonic stem cells. *Biotechnology progress*, 27(6), 1700–1708. *doi*: 10.1002/btpr.675.

Mondragon-Teran, P., Lye, G. J. and Veraitch, F. S. (2009). Lowering oxygen tension enhances the differentiation of mouse embryonic stem cells into neuronal cells. *Biotechnology progress*, 25(5), 1480–1488. *doi*: 10.1002/btpr.248.

Montgomery, D. C. (2012). *Design and Analysis of Experiments* (8 th Edition). *doi*: 10.1198/tech.2006.s372.

Nori, S. et al. (2011). Grafted human-induced pluripotent stem-cell-derived neurospheres promote motor functional recovery after spinal cord injury in mice. *Proceedings of the National Academy of Sciences of the United States of America*, 108(40), 16825–16830. *doi*: 10.1073/pnas.1108077108.

Oburoglu, L. et al. (2014). Glucose and glutamine metabolism regulate human hematopoietic stem cell lineage specification. *Cell Stem Cell*, 15(2), 169–184. *doi*: 10.1016/j.stem.2014.06.002.

Okamoto, S. and Takahashi, M. (2011). Induction of retinal pigment epithelial cells from monkey iPS cells. *Investigative ophthalmology & visual science*, 52(12), pp. 8785–90. *doi*: 10.1167/iovs.11-8129.

Park, I.H. et al. (2008). Disease-Specific Induced Pluripotent Stem Cells. *Cell*, 134(5), pp. 877–886. *doi*: 10.1016/j.cell.2008.07.041.

Park, I. H. et al. (2019). Mitochondria damaged by Oxygen Glucose Deprivation can be Restored through Activation of the PI3K/Akt Pathway and Inhibition of Calcium Influx by Amlodipine Camsylate. *Scientific Reports*, 9:15717.

Robinton, D.A and Daley, G.Q. (2012). The promise of induced pluripotent stem cells in research and therapy. *Nature*, 481(7381):295-.305. *doi*: 10.1038/nature10761.

Stacpoole, S. R. L. et al. (2013). High yields of oligodendrocyte lineage cells from human embryonic stem cells at physiological oxygen tensions for evaluation of

translational biology. *Stem cell reports*, 1(5), 437–450. *doi*: 10.1016/j.stemcr.2013.09.006.

Stolzing, A., Coleman, N. and Scutt, A. (2006). Glucose-Induced Replicative Senescence in Mesenchymal Stem Cells. *Rejuvenation Research*, 9(1), 31–35. *doi*: 10.1089/rej.2006.9.31.

Takahashi, K. and Yamanaka, S. (2006). Induction of Pluripotent Stem Cells from Mouse Embryonic and Adult Fibroblast Cultures by Defined Factors. *Cell*, 126, 663–676. *doi*: 10.1016/j.cell.2006.07.024.

Takahashi, K. et al. (2007). Induction of Pluripotent Stem Cells from Adult Human Fibroblasts by Defined Factors. *Cell*, 107(5), 861–872. *doi*: 10.1016/j.cell.2007.11.019.

Takayama, N. et al. (2010). Transient activation of c-MYC expression is critical for efficient platelet generation from human induced pluripotent stem cells. *The Journal of experimental medicine*, 207(13), 2817–2830. *doi*: 10.1084/jem.20100844.

Tay, J. I. et al. (1997). Human tubal fluid: Production, nutrient composition and response to adrenergic agents. *Human Reproduction*, 12(11), 2451–2456. *doi*: 10.1093/humrep/12.11.2451.

Thielman, J. and Ge, P. (2006). Applying axiomatic design theory to the evaluation and optimization of large-scale engineering systems. *Journal of Engineering Design*, 17(1), pp. 1–16. *doi*: 10.1080/09544820500287722

Tsuji, O. et al. (2010). Therapeutic potential of appropriately evaluated safe-induced pluripotent stem cells for spinal cord injury. *Proceedings of the National Academy of*

Sciences of the United States of America, 107(28), 12704–9. *doi*: 10.1073/pnas.0910106107.

Singh, B. et al. (2005). Optimizing Drug Delivery Systems Using Systematic "Design of Experiments." Part II: Retrospect and Prospects. *Critical Reviews in Therapeutic Drug Carrier Systems*, 22(3), 215–294. *doi*: 10.1615/CritRevTherDrugCarrierSyst.v22.i3.10.

Song, C. et al. (2019). Elevated Exogenous Pyruvate Potentiates Mesodermal Differentiation through Metabolic Modulation and AMPK/mTOR Pathway in Human Embryonic Stem Cells. *Stem Cell Reports*, 13 (2), 338-351. *doi*: 10.1016/j.stemcr.2019.06.003.

Sperber, H. et al. (2015).The metabolome regulates the epigenetic landscape during naive-to-primed human embryonic stem cell transition. *Nature Cell Biology*, 17(12), 1523–1535. *doi*: 10.1038/ncb3264.

Staller, P., Sulitkova, J., Lisztwan, J., Moch, H., Oakeley, E. J., et al. (2003) Chemokine receptor CXCR4 downregulated by von Hippel-Lindau tumour suppressor pVHL. *Nature*, 425: 307–311.

Varum, S. et al. (2011). Energy metabolism in human pluripotent stem cells and their differentiated counterparts. *PLoS ONE*, 6(6). *doi*: 10.1371/journal.pone.0020914.

Vernardis, S. I. et al. (2017). Human embryonic and induced pluripotent stem cells maintain phenotype but alter their metabolism after exposure to ROCK inhibitor. *Scientific Reports*, 7. *doi*: 10.1038/srep42138.

Von Meyenn, F. et al. (2013). Glucagon-Induced Acetylation of Foxa2 Regulates Hepatic Lipid Metabolism. *Cell Metabolism*, 17, 436-447.

Wernig, M. et al. (2008). Neurons derived from reprogrammed fibroblasts functionally integrate into the fetal brain and improve symptoms of rats with Parkinson's disease. *Proceedings of the National Academy of Sciences*, 105(15), 5856–5861. *doi*: 10.1073/pnas.0801677105.

Yagi, T. et al. (2011). Modeling familial Alzheimer's disease with induced pluripotent stem cells. Human Molecular Genetics, 20(23), 4530–4539. *doi*: 10.1093/hmg/ddr394.

Yahata, N. et al. (2011). Anti-Aβ drug screening platform using human iPS cell-derived neurons for the treatment of Alzheimer's disease. *PLoS ONE*, 6(9). *doi*: 10.1371/journal.pone.0025788.

Yang, H. et al. (2016). Effect of a feeder layer composed of mouse embryonic and human foreskin fibroblasts on the proliferation of human embryonic stem cells. *Experimental and Therapeutic Medicine*, 11(6), 2321–2328. *doi*: 10.3892/etm.2016.3204.

Table 1: Markers and primers used to evaluate the gene expression for germ layer formation and pluripotency.

Biomarker	Description	QuantiTect Primer Assay	Catalogue Number	Supplier
β-Actin	House Keeping gene	Hs_ACTB_2_SG	QT01680476	Qiagen
Tubulin 3	Ectodermal marker	Hs_TUBB3_1_SG	QT00083713	Qiagen
Nestin	Ectodermal marker	Hs_NES_2_SG	QT01015301	Qiagen
SOX17	Endodermal marker	Hs_SOX17_1_SG	QT00204099	Qiagen
FOXA2	Endodermal marker	Hs_FOXA2_1_SG	QT00212786	Qiagen
CXCR4	Endodermal marker	Hs_CXCR4_2_SG	QT02311841	Qiagen
Brachyury	Mesoderm marker	Hs_T_1_SG	QT00062314	Qiagen
KIFA	Mesoderm marker	Hs_KIF1A_1_SG	QT00072604	Qiagen

Table 2: Factors and levels used for the Design of Experiments.

Factor	Level		
	Deprivation	**Physiological Environment**	**Laboratory Conditions**
Oxygen (% v/v)	0	2	20
Glucose (mM)	0	3.14	17.50
Pyruvate (mM)	0	0.14	0.50

Table 3: Culture conditions informed by the predictive model to direct differentiation towards a particular lineage via manipulation of oxygen, glucose and pyruvate concentrations

Germ Layer	**Oxygen (%)**	**Glucose (mM)**	**Pyruvate (mM)**	**Desirability**
Endoderm	**20**	**0.10**	**0.5**	**0.61**
Mesoderm	**0**	**0.15**	**0.5**	**0.75**
Ectoderm	**0**	**1.00**	**0.5**	**0.78**

Figure Legends:

Figure 1: Contour maps of the model for endodermal gene expression at days 3 and 4 after differentiation. Gene expression for differentiated iPSCs was assessed by RT-PCR. Colours ranging from dark blue to dark red represent the lowest and highest log value respectively for endodermal gene expression: (A) SOX 17 at day 3, (B) SOX 17 at day 4, (C) CXCR4 at day 3 and (D) CXCR4 at day 4.

Figure 2: Endodermal gene expression for SOX17 (A), FOXA2 (B) and CXCR4 (C) over time at deprivation levels, physiological and laboratory conditions. All RT-PCR data are shown as mean ± SEM (N = 3).

Figure 3: Contour maps of the model for mesodermal gene expression at days 3 and 4 after differentiation. Gene expression for differentiated iPSCs was assessed by RT-PCR. Colours ranging from dark blue to dark red represent the lowest and highest log value respectively for endodermal gene expression: (A) Brachyury at day 3, (B) Brachyury at day 4, (C) KIF1A at day 3 and (D) KIF1A at day 4.

Figure 4: Mesodermal gene expression for Brachyury (A) and KIF1A (B) over time at deprivation levels, physiological and laboratory conditions. All RT-PCR data are shown as mean ± SEM (N = 3).

Figure 5: Contour maps of the model for Nestin gene expression at days 3 (A-C) and 4 (D-F) after differentiation. Gene expression for differentiated iPSCs was assessed by RT-PCR. Colours ranging from dark blue to dark red represent the lowest and highest log value respectively for endodermal gene expression of Nestin.

Figure 6: Contour maps of the model for Tubulin 3 gene expression at days 3 (A-C) and 4 (D-F) after differentiation. Gene expression for differentiated iPSCs was

assessed by RT-PCR. Colours ranging from dark blue to dark red represent the lowest and highest log value respectively for endodermal gene expression of Tubulin 3.

Figure 7: Ectodermal gene expression for Nestin (A) and Tubulin 3 (B) over time at deprivation levels, physiological and laboratory conditions. All RT-PCR data are shown as mean ± SEM (N = 3).

Figure 8: Contour maps of the model for viable cell density of the 27 conditions within the 4 days of differentiation. Cell viability was assessed via the trypan blue exclusion method. Colours ranging from dark blue to dark red represent the lowest and highest value for viable cell count respectively at day 1(A), day 2(B), day 3(C) and day 4(D).

Figure 9: Brightfield micrographs of iPSCs cultured at deprivation levels (A), physiological (B) and laboratory (C) conditions after 4 days of differentiation. Images were taken at 100X ocular magnification using Evos® XL. Scale bars=400µm.

Figure 10: Predictive model for maximum gene expression and cell viability in each germ layer. Colours ranging from dark blue (0) to dark red (1) represent the lowest and highest values for desirability. The dashed area in each model represents the optimum range predicted by the model for endoderm (A), mesoderm (B) and ectoderm (C) germ layers.

Figure 11: Adding glucose to the media retained the endodermal lineage expression of differentiated human episomal iPSCs (Cord blood). Real time PCR was performed in order to assess the fold gene expression of each germ layer: (A) Endoderm (Sox 17, FOXA2, CXCR4), (B) Ectoderm (Nestin,Tubulin 3,Pax6) and (C) mesoderm (Brachyury,KIF1A) for normal and deprived conditions.(D) cell viability was assessed by trypan blue exclusion method.

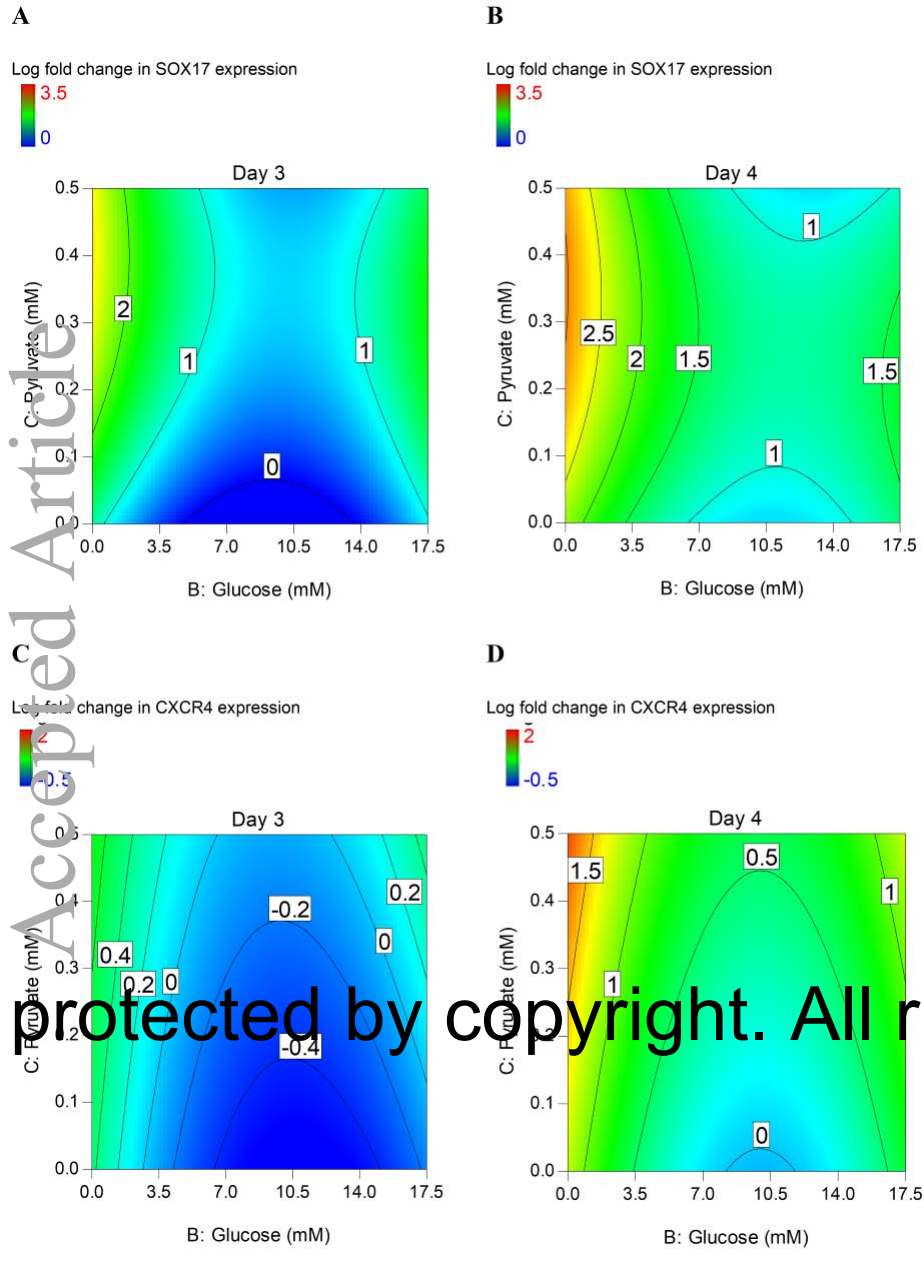

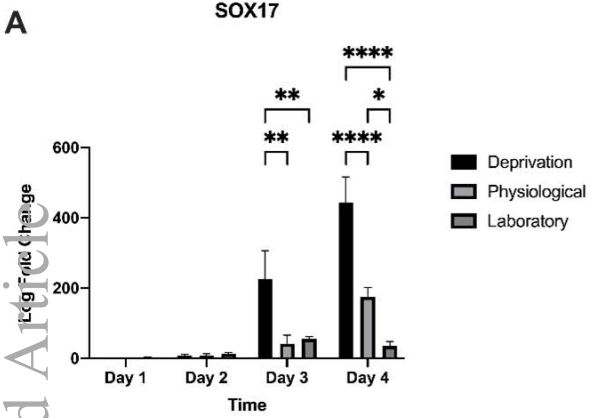

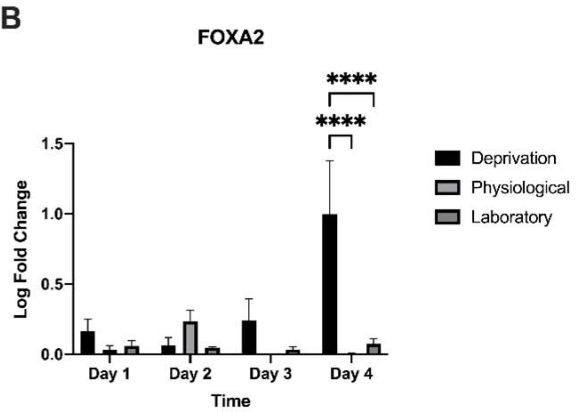

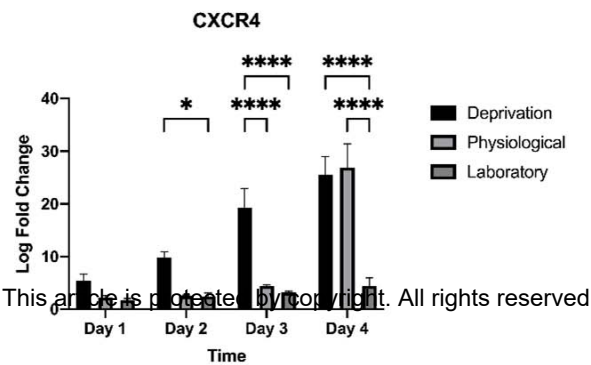

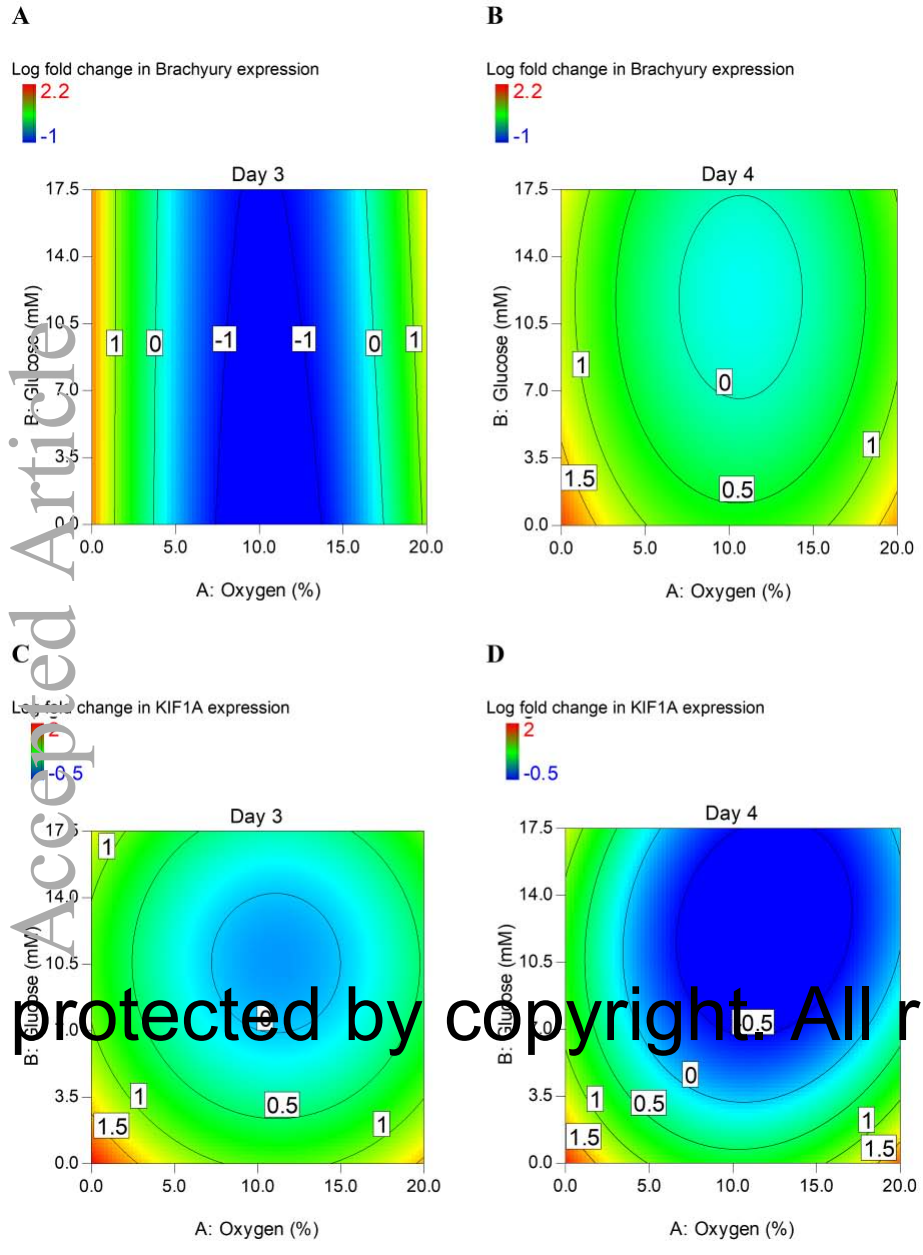

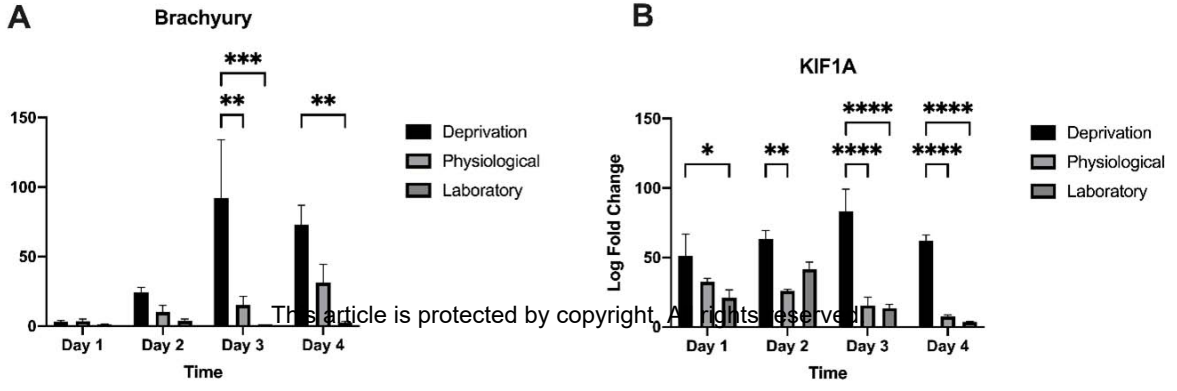

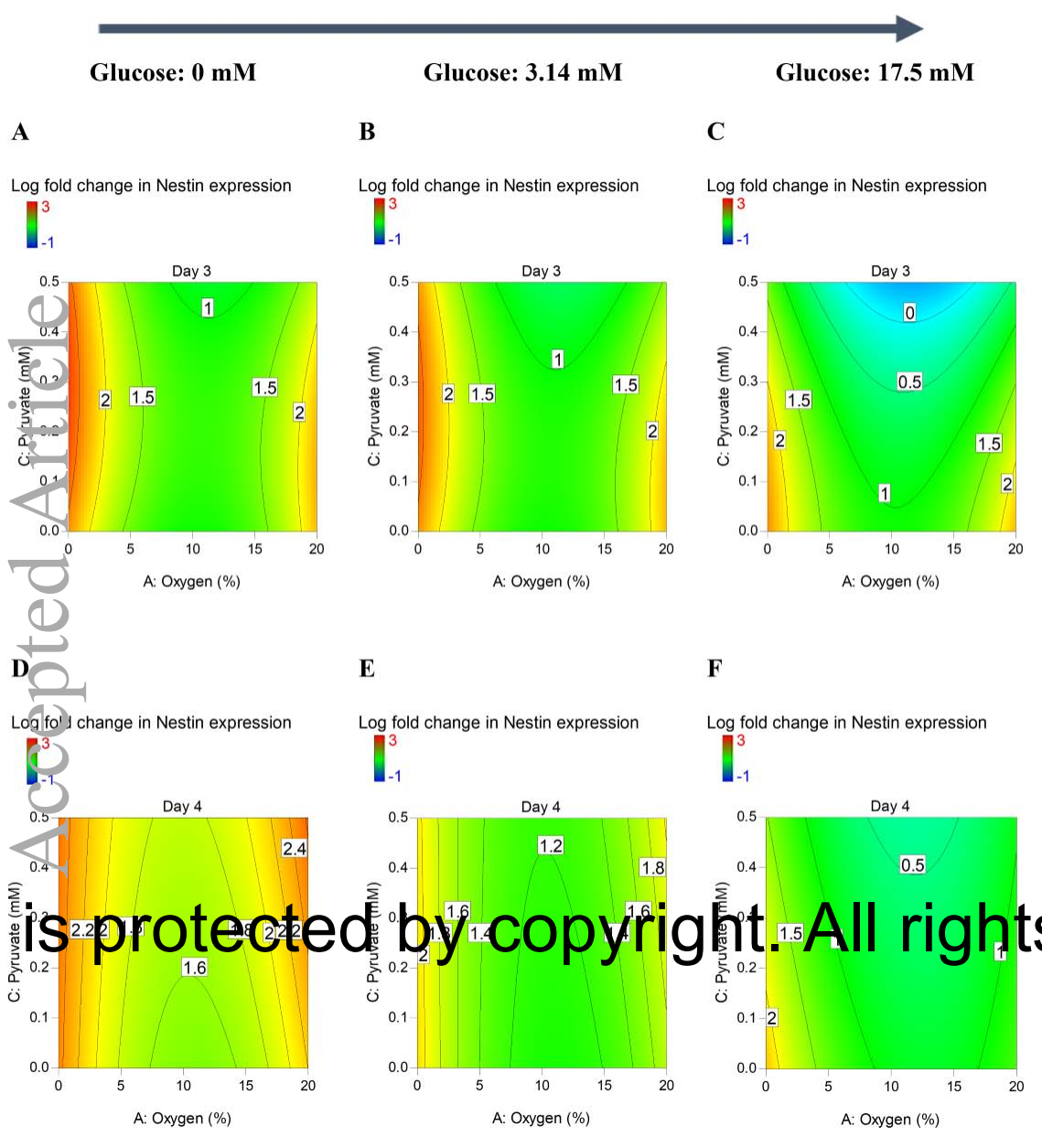

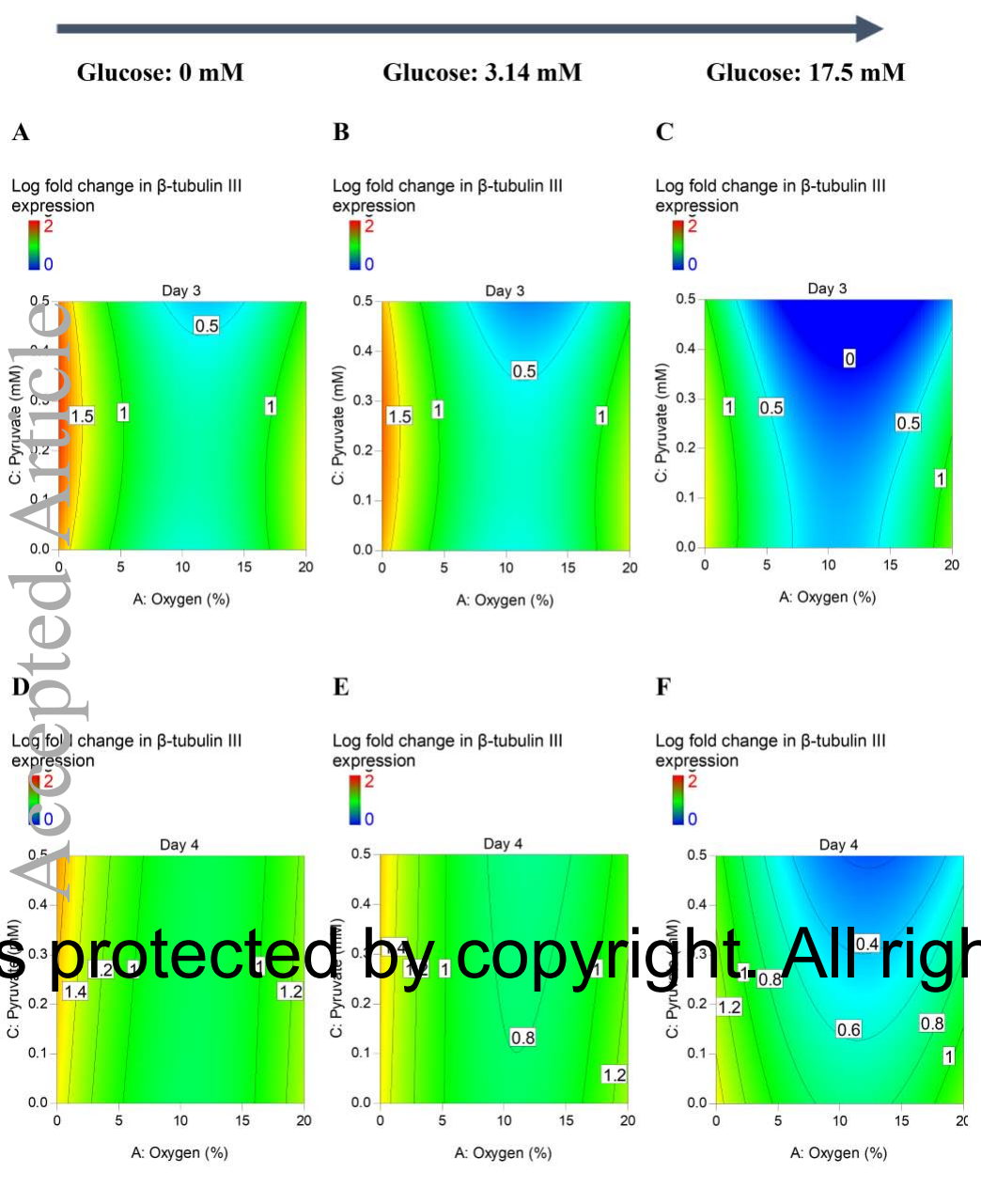

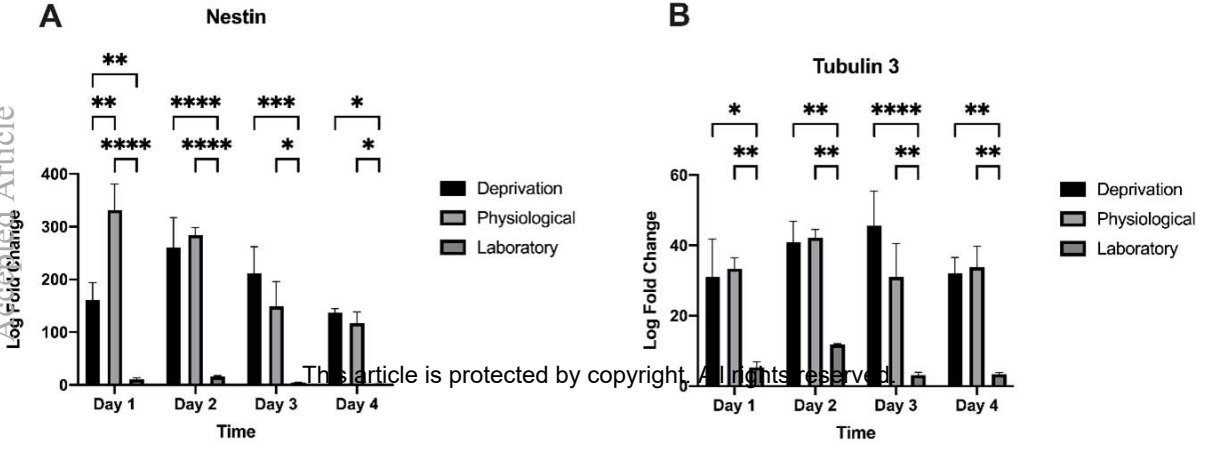

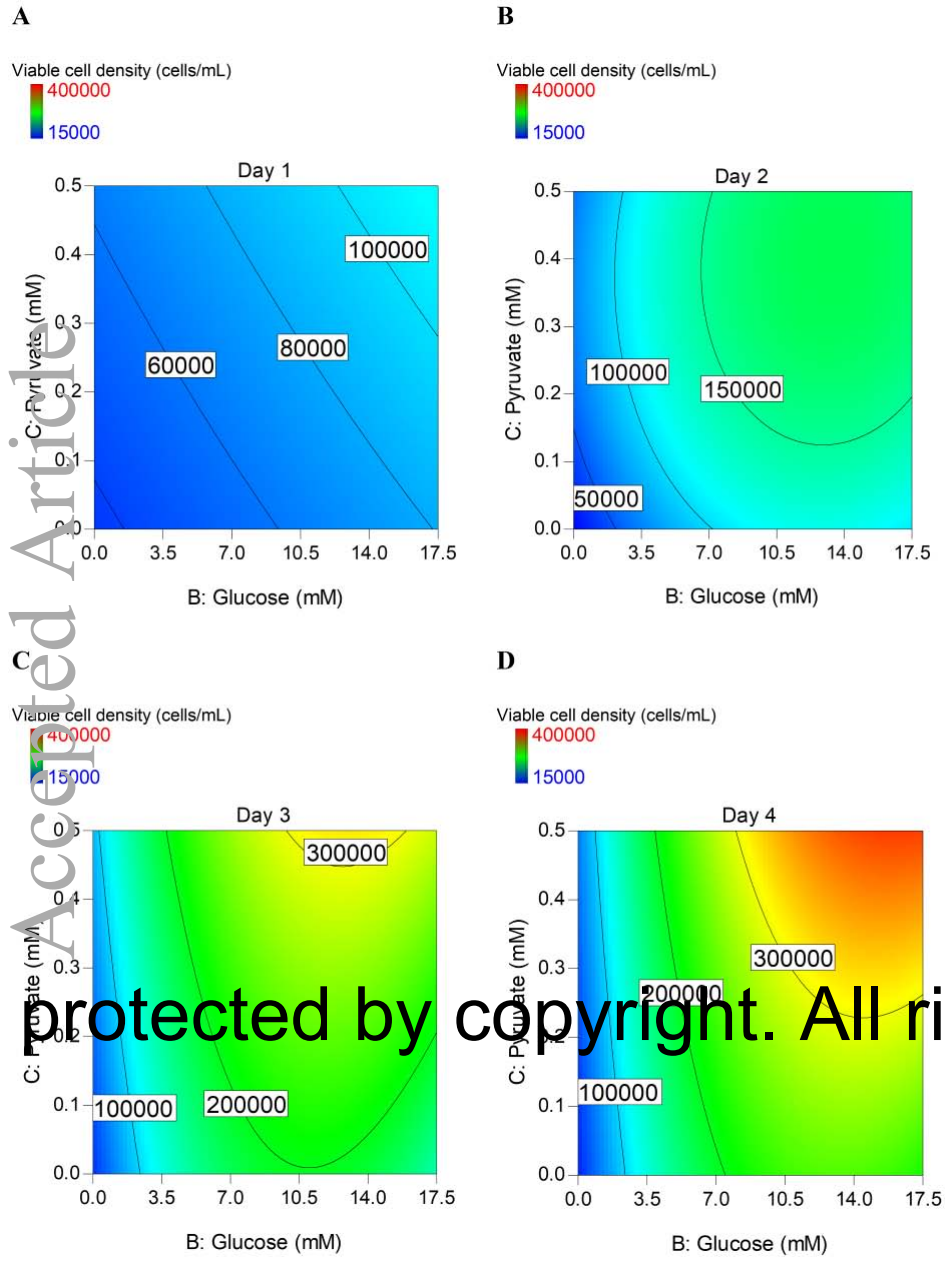

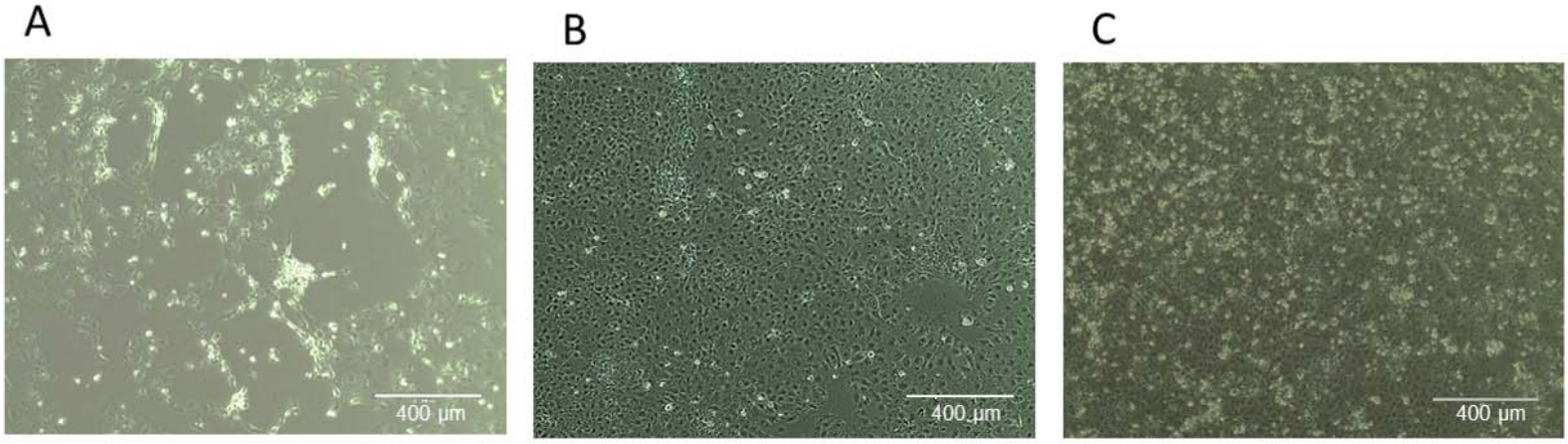

A

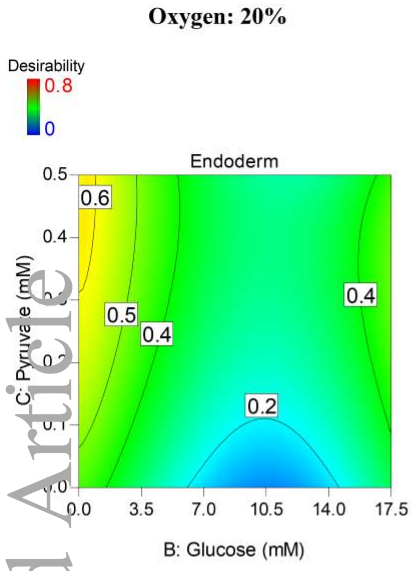

B

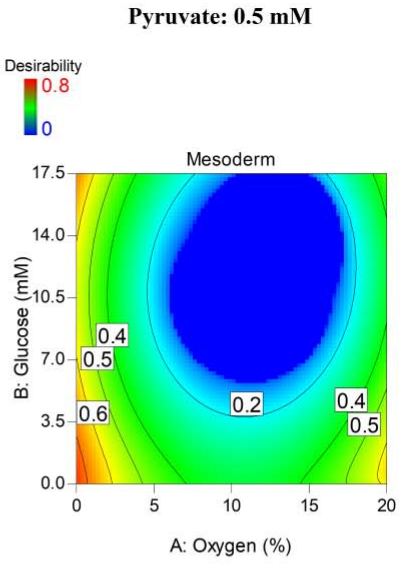

C